ENVIRONMENTAL RESEARCH
LETTERS

LETTER • OPEN ACCESS

An evapotranspiration deficit-based drought index to detect variability of terrestrial carbon productivity in the Middle East

ENVIRONMENTAL RESEARCH
LETTERS

CrossMark

OPEN ACCESS

RECEIVED
4 May 2021

REVISED
15 December 2021

ACCEPTED FOR PUBLICATION
31 December 2021

PUBLISHED
14 January 2022

LETTER

An evapotranspiration deficit-based drought index to detect variability of terrestrial carbon productivity in the Middle East

Karam Alsafadi[1], **Nadhir Al-Ansari**[2], **Ali Mokhtar**[3,4], **Safwan Mohammed**[5], **Ahmed Elbeltagi**[6,7], **Saad Sh Sammen**[8] and **Shuoben Bi**[1,*]

1 School of Geographical Sciences, Nanjing University of Information Science and Technology, Nanjing 210044, People's Republic of China
2 Civil, Environmental and Natural Resources Engineering, Lulea University of Technology, 97187 Lulea, Sweden
3 Department of Agricultural Engineering, Faculty of Agriculture, Cairo University, Giza 12613, Egypt
4 State of Key Laboratory of Soil Erosion and Dryland Farming on Loess Plateau, Institute of Soil and Water Conservation, Northwest Agriculture and Forestry University; Institute of Soil and Water Conservation, Chinese Academy of Sciences and Ministry of Water Resources, Yangling 712100, People's Republic of China
5 Institute of Land Use, Technology and Regional Development, University of Debrecen, Debrecen 4032, Hungary
6 Agricultural Engineering Department, Faculty of Agriculture, Mansoura University, Mansoura 35516, Egypt
7 College of Environmental and Resource Sciences, Zhejiang University, Hangzhou 310058, People's Republic of China
8 Department of Civil Engineering, College of Engineering, University of Diyala, Diyala Governorate 32001, Iraq
* Author to whom any correspondence should be addressed.

E-mail: bishuoben@163.com

Keywords: gross primary productivity, SEDI, ecosystem dynamics, terrestrial carbon, GLEAM dataset

Abstract

The primary driver of the land carbon sink is gross primary productivity (GPP), the gross absorption of carbon dioxide (CO_2) by plant photosynthesis, which currently accounts for about one-quarter of anthropogenic CO_2 emissions per year. This study aimed to detect the variability of carbon productivity using the standardized evapotranspiration deficit index (SEDI). Sixteen countries in the Middle East (ME) were selected to investigate drought. To this end, the yearly GPP dataset for the study area, spanning the 35 years (1982–2017) was used. Additionally, the Global Land Evaporation Amsterdam Model (GLEAM, version 3.3a), which estimates the various components of terrestrial evapotranspiration (annual actual and potential evaporation), was used for the same period. The main findings indicated that productivity in croplands and grasslands was more sensitive to the SEDI in Syria, Iraq, and Turkey by 34%, 30.5%, and 29.6% of cropland area respectively, and 25%, 31.5%, and 30.5% of grass land area. A significant positive correlation against the long-term data of the SEDI was recorded. Notably, the GPP recorded a decline of >60% during the 2008 extreme drought in the north of Iraq and the northeast of Syria, which concentrated within the agrarian ecosystem and reached a total vegetation deficit with 100% negative anomalies. The reductions of the annual GPP and anomalies from 2009 to 2012 might have resulted from the decrease in the annual SEDI at the peak 2008 extreme drought event. Ultimately, this led to a long delay in restoring the ecosystem in terms of its vegetation cover. Thus, the proposed study reported that the SEDI is more capable of capturing the GPP variability and closely linked to drought than commonly used indices. Therefore, understanding the response of ecosystem productivity to drought can facilitate the simulation of ecosystem changes under climate change projections.

1. Introduction

In the last few decades, humanity has faced many challenges in the environmental and agricultural sectors, such as the need for reductions in carbon dioxide emissions (Jardine 2003), climate change (Saavedra *et al* 2009, Dai 2011), drought and water scarcity (Mishra and Singh 2011), and food insecurity (Margulis 2013). The concept of drought as a temporal dynamic phenomenon differs from aridity as a spatial dynamic phenomenon, which results from a decrease in precipitation in a specific area and a remarkable increase in the potential evapotranspiration (PET) rate (Alsafadi *et al* 2020, Elbeltagi *et al* 2021). The time factor or the length of the drought period is considered one of the most important criteria for determining the severity of drought risk (Mokhtar *et al* 2021a). The issue of drought and its spatial consequences have often been the focus of studies carried out in the Middle East (ME) ecosystem (Kaniewski *et al* 2012, Hameed *et al* 2020). In recent decades, drought has turned into one of the most severe natural disasters for the ME's ecosystem in the context of global climate change (Lelieveld *et al* 2012, Mohammed *et al* 2020b). Moreover, drought has significantly affected terrestrial ecosystems, economic, social and political systems in the ME, including food security (Hameed *et al* 2020), hydrological processes (Bozkurt and Sen 2013), vegetation growth (Zaitchik *et al* 2007, Karakani *et al* 2021) and the extinction of many plant species (Belgacem and Louhaichi 2013). Generally, the ME's ecosystem is classified as a transitional climate pattern, located between a hot-dry and cold-humid climate pattern, which is most exposed to drought events as a result of prolonged water shortages. The ME is a crucial region for comprehension of drought globally (Barlow *et al* 2016).

As a result of the close relationship between ecosystem dynamics and available water, a water deficit can be restrictive to ecosystem growth (Yi *et al* 2010, Mokhtar *et al* 2021b). Thus, ecosystem conditions can reflect drought risk; for instance, both precipitation and temperature changes significantly affect the ecosystem (Mokhtar *et al* 2020, Mohammed *et al* 2020a). Precipitation plays a vital role in controlling the productivity of the grass; increasing precipitation results in increasing grass productivity while, in contrast, the grass lands are critically impacted by temperature (Li *et al* 2013, Lei *et al* 2015). Indeed, biogeochemical carbon cycles of the ecosystem reflect the atmosphere conditions and serve as an indicator of climate change (Piao *et al* 2005, Xu *et al* 2009). Drought is one of the main factors impacting ecosystems' distribution patterns and types (Vicente-Serrano *et al* 2012, 2015). Several studies have documented that ecological programs can reduce ecosystem degradation and enhance vegetation coverage, although these programs did not work well (Deng *et al* 2014, Wu *et al* 2014, Zhang *et al* 2015b). Further, afforestation of semiarid areas results in ecosystem degradation due to the impact of drought and human activity on ecosystem change (Cao 2008, Huang *et al* 2016a).

Consequently, vegetation conditions are positively and negatively correlated with precipitation in dry and wet regions, respectively (Prasad and Staggenborg 2008, Jiao *et al* 2019a). In previous studies, experimental methods, satellite observations, and carbon process models have documented that large-scale droughts reduce the vegetation activity, and severe temperatures lead to negative terrestrial carbon productivity even under mild drought conditions (Zhao *et al* 2010, 2013, Stocker *et al* 2019). Droughts impact ecosystem productivity by restricting vegetation growth stages, including a wide range of tree mortality and ecosystem fire, and can influence the global CO_2 balance (Chen *et al* 2013, Reichstein *et al* 2013, Yu *et al* 2017, Jiao *et al* 2021).

Understanding the response of terrestrial ecosystems to drought remains challenging because of the biochemical and physiological activities of vegetation growth and cultivated crops, especially their CO_2 assimilation and ecosystem carbon dioxide fluxes that are constrained by varying degrees of drought at various timescales (Sun *et al* 2021).

Several evapotranspiration-based indices were established to quantify drought and its impacts on terrestrial ecosystems, including Palmer drought severity index (Palmer 1965), Reconnaissance drought index (RDI) (Tsakiris and Vangelis 2005), the standardized precipitation evapotranspiration index (SPEI) (Vicente-Serrano *et al* 2010a) and the evaporative drought index (EDI) (Yao *et al* 2010), the drought severity index (Mu *et al* 2013). Also, there are dozens of drought indices, such as the standardized precipitation index (McKee *et al* 1993), vegetation growth anomaly-based drought indices e.g. vegetation condition index (Liu and Kogan 1996) and vegetation health indices (Kogan 2002), soil moisture deficit index (Narasimhan and Srinivasan 2005), scaled drought condition index (Rhee *et al* 2010), the process-based accumulated drought index (Zhang *et al* 2017a), integrated drought index (IDI) (Jiao *et al* 2019b), and microwave IDI (Zhang *et al* 2019a).

In light of the findings of previous studies, the AET and PET-based drought indices significantly highlight the intensity of water deficits and the influence on vegetation activities more than the individually based indices (Zhang *et al* 2019c). As such, Kim and Rhee (2016) suggested a standardized evapotranspiration deficit index (SEDI), and concluded that the SEDI helps detect agricultural drought events with strong land-atmosphere interactions. Zhang *et al* (2019c) applied the SEDI to investigate the impact of water stress on vegetation growth under global warming and documented the strong interaction between vegetation and the evapotranspiration deficit (ED). Consequently, the SEDI is based on the evaporative stress perspective, which is more directly linked to vegetation water stress than other drought indices (Zhang *et al* 2019c). The PET reflects the atmospheric potential to receive water or evaporative demand. The PET regulates soil water stress conditions, while the actual evapotranspiration (AET) is the amount of water lost from an ecosystem induced by evaporation and transpiration. From eco-physiological and agricultural perspectives, the ED is the difference between the AET and the PET (Vicente-Serrano *et al* 2018). Under climatic stress, a high ED results in stomatal closure, which decreases the photosynthetic process, carbohydrate accumulation, and terrestrial ecosystem production (NPP and GPP) (Stephenson 1998, Eamus 2003).

Based on the above, we used a correlation analysis between the standardized GPP residual series and SEDI to investigate the drought variability and ecosystem response. This research is focused mainly on 35 years for both GPP and SEDI over the ME. Consequently, this research aims to improve the understanding of the correlation between evaporation deficit-based drought and ecosystem vegetation and detect the response of national-level GPP to drought in different land-cover types. As such, the principal aims of this research are: (a) quantify the spatial-temporal variability of GPP dynamics in response to drought at the pixel scale and for each land cover type separately, (b) analysis of ecosystem resilience to drought events of several types, and assessment of an ecosystem's capability to tolerate drought event disturbances, and (c) prove that the ED-based index is more capable of capturing the standardized GPP residuals (sGPPR) variability and closely linked to drought than commonly used indices based on variables other than ED.

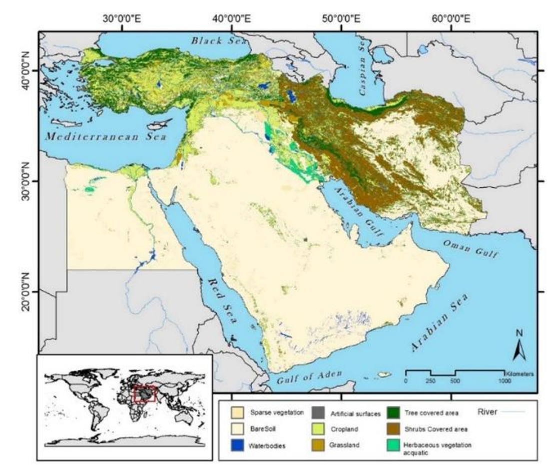

Figure 1. Location of the study area and land cover map, from the GLC-SHARE database (FAO 2014).

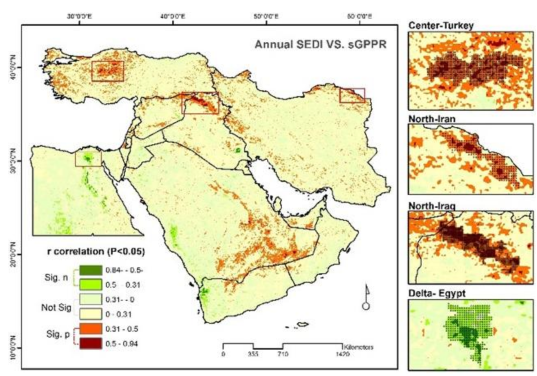

Figure 2. Spatial correlation between the GLASS-based sGPPR and annual SEDI series from 1982 to 2017. The bold colors of red and green denote the r significant correlations i.e. significant positive correlation (Sig p) and significant negative correlation (Sig n), while, the light colors of red and green indicate the r not significant (Not Sig), at a 0.05 significance value (95% confidence interval) and a 0.31 critical correlation value.

2. Materials and methodology

2.1. Study area

The ME is located in the western part of Asia and northeast of Africa, between 12° 06′ N and 42° 07′ N latitudes, and 24° 41′ E and 63° 17′ E longitudes (figure 1). The ME officially includes 16 countries: the Arabian Peninsula region includes Bahrain, Kuwait, the Sultanate of Oman, Qatar, Saudi Arabia, the United Arab Emirate, and Yemen, and the Levant includes Jordan, Lebanon, Palestine, and Syria. Included as well are Egypt, Iran, Iraq, Israel, and Turkey. The ME covers an area of 6928 thousand km^2, inhabited by about 357.23 million people according to World Bank's 2019 statistics (World Bank 2020) and according to the FAO Global Land Cover SHARE database (FAO 2014). The ME's land cover type is mostly bare soil lands, at 61%. However, the whole area of Turkey, northeastern Iraq, western Iran, western and northwestern Syria, most parts of Lebanon, and around the Nile River in Egypt are dominated by grasslands, shrublands, and croplands. In contrast, forests cover northern and southern Turkey and the north and western parts of Iran (see figure 2).

2.2. Ecosystem gross primary productivity (GPP) data

To quantify the sensitivity of GPP against SEDI, we evaluated four state-of-the-art GPP datasets based on Earth observation data as following:

(a) The yearly GLASS-GPP (the Global Land Surface Satellite) dataset, specifically the latest version spanning 35 years between 1982 and 2017 (Zheng et al 2020). The GLASS-GPP dataset was derived from the Eddy Covariance—Light Use Efficiency model (Yuan et al 2007). The latest version of the yearly GLASS-GPP dataset is available globally at 0.05° arc degree spatial resolution within the GLASS products (www.glass.umd.edu).

(b) The ensembled monthly FLUXCOM-GPP, specifically the FLUXCOM-RS + METEO spanning 34 years between 1982 and 2016 (Tramontana et al 2016, Jung et al 2020). The ensembled FLUXCOM-GPP dataset was derived from satellite data and daily meteorological data. This version of the monthly FLUXCOM-GPP dataset is available globally at 0.5° arc degree spatial resolution within the FLUXCOM portal (www.fluxcom.org).

(c) The yearly GIMMS-GPP (Global Inventory Modeling and Mapping Studies), specifically the updated version (version 4) that extend from 1982–2016 (Smith et al 2016). The monthly GIMMS-GPP dataset is available globally at 0.5° arc degree spatial resolution.

(d) The yearly VPM-GPP data (the vegetation photosynthesis model) that extends from 2000 to 2016 (Zhang et al 2017b). The yearly VPM-GPP dataset is available globally at 0.5° arc degree spatial resolution (https://doi.org/10.6084/m9.figshare.c.3789814).

2.3. AET and PET

To quantify the SEDI, the Global Land Evaporation Amsterdam Model (GLEAM, version 3.3a) dataset, spanning 35 years (1982–2017), was used (Miralles et al 2011, Martens et al 2017). The GLEAM dataset gives estimates based on remotely sensed observations to set algorithms that predict the various components of terrestrial evapotranspiration separately. They include transpiration, open water evaporation, bare soil evaporation, sublimation, and interception loss. We used annual AET and PET estimates (mm yr^{-1}) to calculate the SEDI. The GLEAM datasets are currently available within the GLEAM portal at daily, monthly and annual temporal resolution, and at 0.25° arc degree spatial resolution for 1980–2018 (NETCDF files) (www.gleam.eu).

3. Methodology

3.1. The SEDI calculation

For all gridded points of more than 28 000 pixels for 1982–2017 at the annual scale, the SEDI was calculated (Alsafadi and Bi 2021). In this study, the SEDI was implemented as the standardized difference between AET and PET. This was similar to Zhang et al (2019c), as shown:

$$\mathrm{SEDI} = \frac{\mathrm{ED} - \mathrm{ED}_{\mathrm{avg}}}{\mathrm{ED}_{\mathrm{std}}}, \mathrm{ED} = \mathrm{AET} - \mathrm{PET}, \quad (1)$$

where ED is the AET and PET difference (mm yr^{-1}) and $\mathrm{ED}_{\mathrm{std}}$ and $\mathrm{ED}_{\mathrm{avg}}$ denote the standard deviation and multi-years mean, respectively. This can highlight dry and wet conditions by tracking local water storage changes within the soil, compared with direct evaporation.

3.2. Standardized GPP residual series (sGPPR)

Normally, the contributions of human activities to variations in vegetation are removed to detect climate elements impacts independently, calculated by the residuals of the vegetation trend models by computing the de-trended analysis. Since the GPP series is affected by many variables besides climate factors, often, the annual GPP series has a positive trend specifically over agricultural systems and forests. The sGPPR series was obtained from the mean μ and standard deviation value σ of deference between the GPP value and its de-trended value for each year separately, from 1982 to 2017 at the pixel scale (Alsafadi and Bi 2021). The sGPPRS was calculated as:

$$\mathrm{sGPPRS} = \frac{y_i^{(T)} - \mu}{\sigma} \quad (2)$$

$$y_i^T = y_i^0 - y_i^{(\tau)} \quad (3)$$

where (y_i^0) is the observed GPP and $(y_i^{(\tau)})$ is the value of the de-trended GPP in a separate year. The GPP, de-trended during the period of 1982–2018, was calculated for each pixel (more than 23 000 series) using a simple linear regression (SLR) analysis, by using the ordinary least square method, OLS, which was calculated as:

$$y_i^{(\tau)} = \partial + x_i\beta. \quad (4)$$

Herein, we assumed the temporal evolution (x_i) from 1982 to 2017 is an independent variable, and the GPP series data a dependent variable (y_0), to fit the SLR or the value of the de-trended GPP in a separate year

$$\beta = \frac{n \times \sum_{i=1}^{n} x_i \times y_i^0 - \sum_{i=1}^{n} x_i \sum_{i}^{n} y_i^0}{n \times \sum_{i=1}^{n} x_i^2 - \left(\sum_{i=1}^{n} x_i\right)^2} \quad (5)$$

$$\partial = \bar{y}_n^0 - \beta \bar{x}_n \quad (6)$$

where n is the length of the studied period, while β is the slope ratio or annual change of GPP (g m^2 yr^{-1}) acquired by the ordinary least square method. $\beta < 0$ indicates that the GPPs tended to decrease over the studied years, and vice versa. The sGPPR dataset is openly available in Zenodo repository (Alsafadi and Bi 2021)

Pearson's correlation coefficient (r) was used to assess the temporal consistency of the observed GPP and SEDI across the time series.

4. Results

4.1. Assessment of SEDI impacts on GLASS-based sGPPR across terrestrial biomass

In order to quantify the sensitivity of GPP to the SEDI in different land-cover types, the yearly GLASS-GPP at 0.05° arc degree spatial resolution was used, since it has sufficient spatial resolution unlike than that of the other products.

Based on the ecosystem map analysis, we further evaluated the impact of the SEDI on ecosystem productivity from 1982 to 2017. The correlation between the GLASS-based sGPPR and annual SEDI for the ME (figure 2) and each ecosystem type is shown in figure 3. The strongest significant positive correlation was presented in the central portion of the study area, especially in the north of Iraq and central area of Turkey, as well as some portions of northern Iran

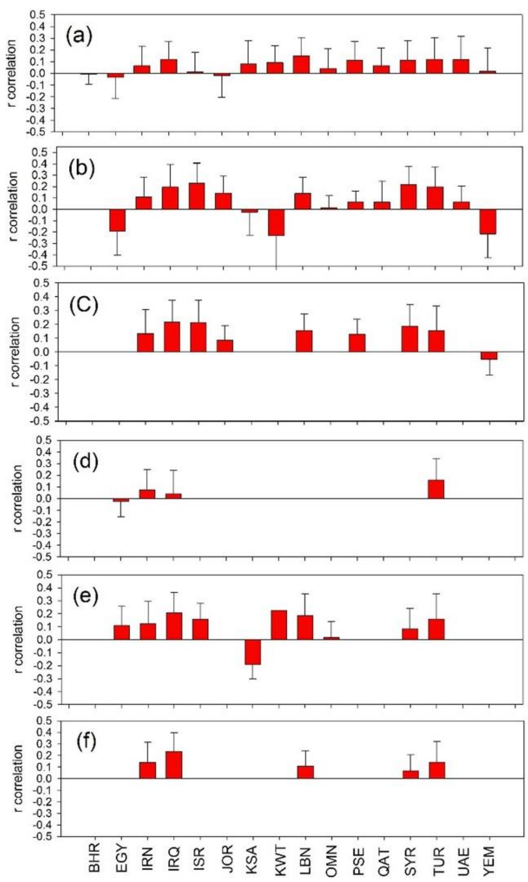

Figure 3. The spatial correlation between the GLASS-based sGPPR and annual SEDI from 1982 to 2017 for each land cover types: (a) bare land; (b) croplands; (c) grasslands; (d) aquatic vegetation; (e) shrubs covered area; (f) tree covered area. The vertical line denotes the standard deviation of the r correlation. The critical value is 0.31 at a 0.05 significance value.

which reached more than 0.5 ($p < 0.05$). Based on table B1, the significant positive correlation areas of crops, grass, tree covered area and shrubs area in Iraq covered 29.6%, 30.6%, 32.4%, and 28.3% of the total area for each cover type, respectively.

The highest significant positive correlation was recorded in the crops ecosystem at 34% of its total area in Syria. The spatial correlation between the GLASS-sGPPR and annual SEDI for each ecosystem type is shown in figure 3. The croplands and grasslands' productivity had the highest positive correlation with the SEDI for several of the study area's countries, especially Iraq, Israel, Syria, and Turkey. Hence the cropland and grassland were more sensitive to SEDI variability.

In contrast, a significantly negative correlation between the sGPPR and annual SEDI was observed over Israel and Jordan for bare land, and the sGPPR of crops vegetation and the annual SEDI was negatively correlated over Egypt and Yemen; 27.2% of this area in Egypt had a significant negative correlation (figure 2). Table B1 and figure 3 demonstrate that the tree-covered area had a significantly positive correlation for the studied countries, especially in Iraq and Turkey at 32.4% and 21.3% of the total area.

Moreover, Turkey, Iraq, and Lebanon achieved the highest percentage of shrubs covered area, with a significantly positive correlation of 31.8%, 28.3%, and 23.8%, respectively. In contrast, the KSA recorded the highest values of significantly negative correlations for the same ecosystem type of 15% (table B1 and figure 3). For sGPPR of the sparse vegetation land in Palestine, Iraq, Turkey, Syria and Iran generated significantly positive correlations with the SEDI of 32.5%, 20%, 18.8%, 16.7%, and 16.1%, respectively. In contrast, the KSA recorded a significantly negative correlation of 30.9% compared to other countries. The aquatic vegetation versus the SEDI produced a significantly positive correlation of 29.4% and 10.4% in Turkey and Iran, respectively, while Iraq reached 5.4% for a highly negative correlation. The sGPPR in the soil bare ecosystem was highly positively correlated with the SEDI in Lebanon and in the UAE, at 22.5% and 20.1%. On the other hand, 7.1% and 7% of the soil bare was highly negatively correlated in Egypt and Jordan (table B1).

4.2. Performance of SEDI in detecting response of the sGPPR dataset to dry and wet climatic condition

This section aimed to prove that the ED-based index is more capable to capture the sGPPR variability and closely linked to drought than commonly used indices based on variables other than ED. Herein, we assessed the performance of SEDI against SPEI in detecting drought effects on terrestrial carbon productivity, using four state-of-the-art GPP dataset.

At the regional scale, we assessed the sensitivity of sGPPR data to the evolution of drought for each index separately. Figure 4 indicates the spatial distribution of correlation values between the four sGPPR datasets and the SEDI from 1982 to 2016. The correlation values between sGPPR and the SEDI in the study area were 0.5, 0.41, 0.3, and 0.2 for the FluxCom, VPM, GIMMS and GLASS models, respectively. In contrast, the correlations between the SPEI and sGPPR were lower with the values of 0.35, 0.23, 0.15, 0.16 for the same models respectively. The spatial distribution patterns of correlations between the SEDI and sGPPR were similar between the SPEI and sGPPR, but higher in the first pattern, which indicates that SEDI can detect stronger response from terrestrial processes, specifically the northern part. The strongest significant positive correlations were presented in the central portion of Turkey, north Iraq, and the western part of Iran and some portions of northern Iran, which reached more than 0.7 ($p < 0.05$) for the FluxCom and VPM models against the SEDI.

4.3. Extreme drought-induced GPP anomaly

As presented in figure A1, the ME's terrestrial ecosystems have experienced drought events, as presented

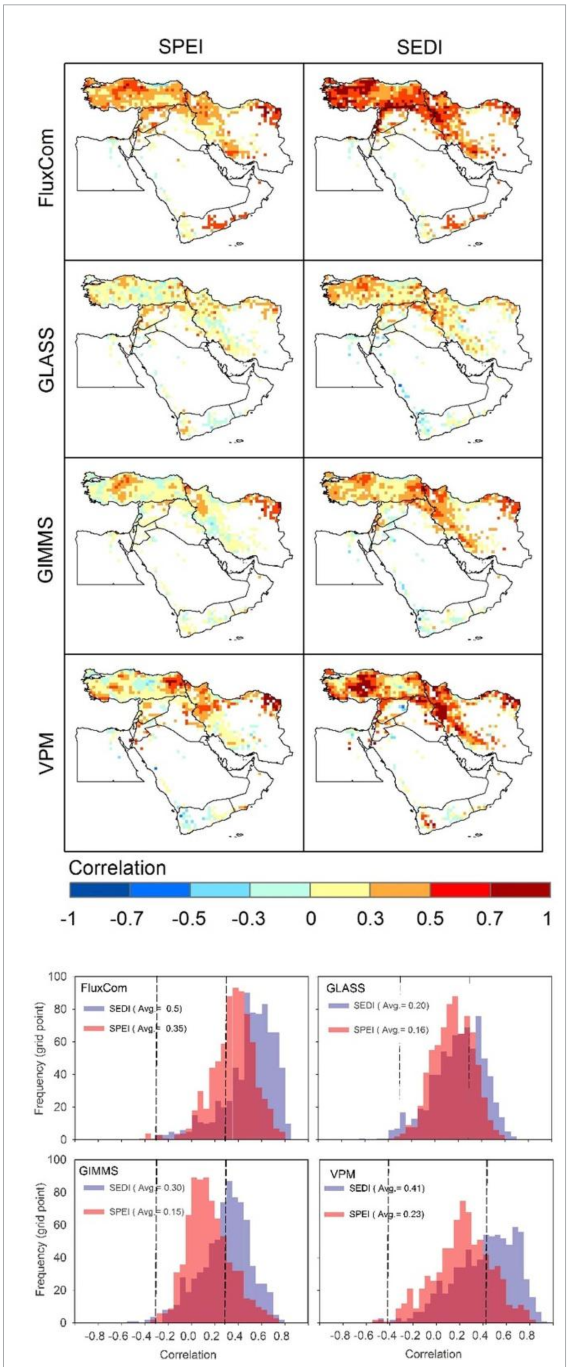

Figure 4. Spatial correlation between the four state-of-the-art sGPPR dataset and standardized drought indices (SPEI and SEDI) from 1982 to 2016 for FluxCom, GLASS and GIMMS and from 2000 to 2016 for VPM. The charts below indicate to the spatial frequency of the correlations at the grid points scale. Note: we used December values of the SPEI-12 timescale spanning 1982–2016 based on the SPEI base v2.6 products (Beguería *et al* 2010, 2014, Vicente-Serrano *et al* 2010b) which are available within the Global SPEI portal at 0.5° arc degree spatial resolution (https://spei.csic.es/database.html).

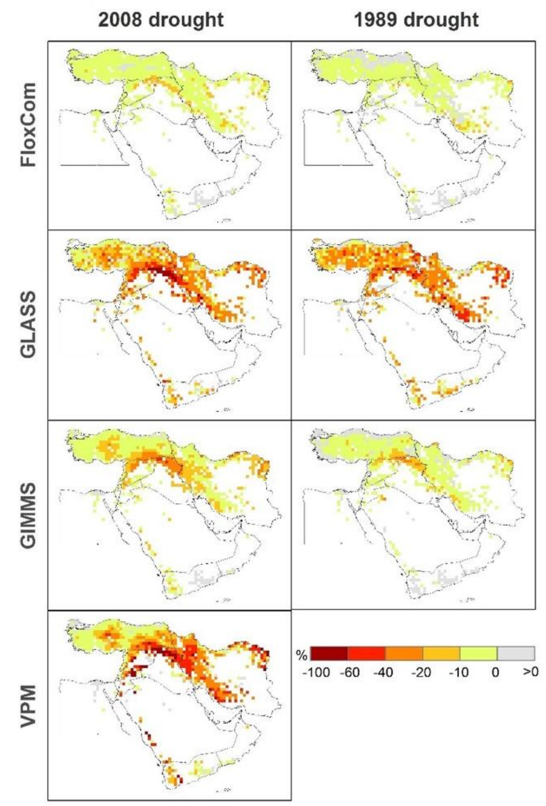

Figure 5. Extreme drought-induced GPP anomaly (%) in the ME for 1989 and 2008.

by SEDI droughts, for the studied period. These have extensively hit terrestrial ecosystems from 1989 to 1990 and 2008 and 2012. The 1989 and 2008 GLASS-GPP anomalies showed high losses in GPP (figure A2). They were somewhat correlated with the annual SEDI in the same years, resulting in a clear reduction in annual GPP, specifically in the Fertile Crescent in Iraq and Syria, by 20%–60%, and higher than that in some parts. The GPP accounted for a high decline of >60% during the 2008 extreme drought (peak of drought) in the north of Iraq, the northeast of Syria, and southwest of Iran (figure 5).

The strongest reductions in annual GPP during 2008 extreme drought were presented for the GLASS and VPM models for the study area. They constituted 20% and more than 60% in some parts, while the GIMMS and FLUXCOM models-based GPP negative anomalies during the drought stress were lower than that of other GPP data and had low spatial variability. The anomalies in annual GPP from 2009 to 2012 might have resulted from a notable decrease in the annual SEDI at the 2008 extreme drought event (figures A1 and A2). After that, the moderate and slight drought from 2009 to 2012 resulted in persistent stress to vegetation, as observed via negative anomaly values of the GPP. Ultimately, this led to a long delay in restoring the ecosystem in terms of its vegetation cover.

5. Discussion

5.1. Sensitivity of GPP data to the evolution of SEDI

The results of this study have shown that spatial-temporal variability of SEDI significantly impacted the GPP models at the pixel scale in the ME. Moreover the SEDI is more capable of capturing the GPP variability than the SPEI. Regarding the SEDI structure, the PET regulates the soil water stress conditions, while the AET is the amount of water lost from an ecosystem induced by both evaporation and transpiration. This is considered an indicator for the physiological activities of vegetation. Regarding agronomic and eco-physiological terrestrial systems, the ED can explicitly account not only for the atmospheric evaporative demand, and also the water transferred to the atmosphere from the soil and vegetation which physiologically explains the vegetation behavior and activity (Kim and Rhee 2016, Vicente-Serrano *et al* 2018, Zhang *et al* 2019c). The soil moisture deficits could result in a stomatal closure to avoid additional water deprivation. If the deficits become high enough to reduce soil moisture below the wilting point, plants will be under stress and may die as a result of vascular damage (Anderegg *et al* 2015). Therefore, the SEDI helps detect agricultural drought events in areas that have a strong land-atmosphere interaction and has a proven high performance in vegetation–drought interactions (Zhang *et al* 2019c).

5.2. Responses of vegetation activity to SEDI

The GPP for the ecosystem in the ME at annual scale showed a moderate correlation with the SEDI during the studied period. However, cropland and grassland were more sensitive to the droughts than other vegetation ecosystem types, these results consistent with previous studies (Pei *et al* 2013, Xiaobin *et al* 2014, Sun *et al* 2016). The maximum correlation for grass and croplands' GPP against the SEDI was in Iraq, Iran and Syria. In a similar context, Huang *et al* (2016b) found that the semi-arid ecosystem types have an essential role in inter-annual NPP variability during long-term droughts. The highest positive correlations between yearly NPP and SPEI were recorded in shrub-covered land, followed by cropland. The results identified that a slight correlation with the SEDI during the studied period was detected in the tree-covered area throughout the northern and northeastern of the study area. It has been suggested that forests productivity may be more resilient to drought events than other ecosystem types due to deeper forest root system compared with grasslands and can access water from a deeper soil profile (Teuling *et al* 2010, van den Hoof and Lambert 2016).

On the other hand, the results indicated that ED driven-drought events positively impacted the GPP of irrigated cropland and herbaceous vegetation aquatic over a large area on both sides of the Nile river and Egyptian Delta as presented in figure 6. Under several management practices of irrigation, it is demonstrated that the variation caused by the role of vegetation respiration in the terrestrial carbon sink. Moreover the higher increment in GPP may be coupled with the higher rate of respiration to GPP during drought conditions, heat waves, and increament of temperature in the atmosphere all these increases the rate of respiration to GPP (Schwalm *et al* 2010, Williams *et al* 2013). Hence, a slight water deficit under irrigation practices will not have an effective role in vegetation productivity losses compared to a high ratio of vegetation respiration. As presented previously, the vegetation productivity in semi-arid lands was more negatively affected by drought than arid and desert land (Zhu *et al* 2021). Example is the Western Desert in Egypt, central part of Iran and the Empty Quarter desert in the KSAs.

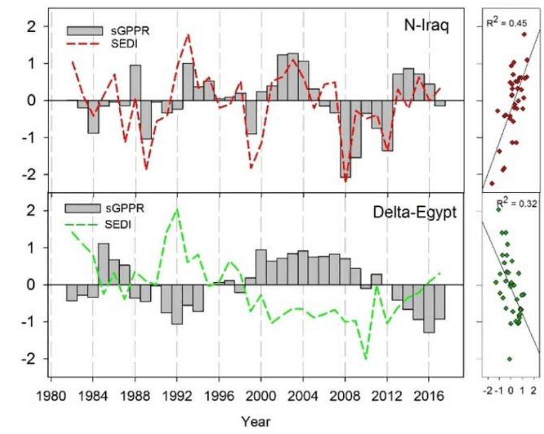

Figure 6. The regional mean of sGPPR and SEDI for different regions (semi-arid ecosystem like north Iraq and irrigated croplands on both sides of the Nile river and Egyptian Delta). R^2 is the determination coefficient.

5.3. Extreme drought-induced GPP anomaly in the ME

Overall, extreme drought is a critical driver of annual and inter-annual variability in continental and regional terrestrial gross and net primary productivity (Ciais *et al* 2005, Schwalm *et al* 2012, Liu *et al* 2014). This research indicated that the ME drought spells and heat waves in 1989 and 2008 over northern and northeastern reduced the carbon cycle, with strong anomalies at regional scale (0.3 and 0.12 PgC yr^{-1}), i.e. a reduction by 20% and 9% of GPP respectively. Notably, the 1989 and 2008 GPP anomalies have been coupled with high evaporation deficits, as presented by the SEDI, and were somewhat correlated with the annual SEDI in the same years, resulting in a clear reduction in the annual GPP specifically in the Fertile Crescent in Iraq and Syria by 40%–60% in 2008. The GPP accounted for a high decline of >60% during the 2008 extreme drought (peak of drought) in the north of Iraq, the northeast of Syria, and the southwest of Iran, as presented in the GLASS and VPM models (figure 6). In general, the GPP is highly sensitive to drought conditions than ecosystem respiration, whereas it is less sensitive than NPP (Schwalm *et al* 2010). For instance, over the Southern United States, the drought intensification is resulted in a significant decrease in NPP, with the highest decrease of 40% occurring during drought of 2000–2004 (Chen *et al* 2012). The incompatibility between the response of GPP and NPP is due to the role of vegetation respiration in the terrestrial carbon sink. Vegetation respiration is less impacted by drought spells than photosynthesis (Schwalm *et al* 2010), and the higher reduction in NPP may be coupled with the higher rate of respiration to GPP during drought conditions, the land and atmosphere increase in temperature increases the rate of respiration to GPP (Green *et al* 2019).

5.4. Uncertainties in analysis and finding

In our study, comparisons between GPP models and SEDI suggested that all of the GPP datasets significantly responded to the dry-wet climatic condition of the SEDI at an annual time-scale. Even though the patterns of the correlations between SEDI and various GPP dataset were similar, but the proportions of responses were extremely varied among the GPP data, could be caused by uncertainties in the GPP data rather than in the SEDI data. It is still hard to simulate GPP at global and regional levels. This limitation in GPP data may cause uncertain interpretations when evaluating the impacts of drought stress on GPP using a few or different GPP products (Liu *et al* 2019). Many remotely sensed GPP datasets are presently available and have been extensively utilized at different spatial-temporal scales (Zheng *et al* 2020). However, either GPP estimates from remote sensing, process-based models, or machine learning methods should be carefully used when assessing GPP response to drought.

The correlations between FLUXCOM-GPP and the SEDI were higher than that of other GPP data in the ME. At the same time, the FLUXCOM model-based GPP negative anomalies during the drought stress were lower than that of other GPP data and had low spatial variability. The flux tower observation-based upscaling data (e.g. the FLUXCOM GPP based on machine learning) can be regarded as observation-based GPP estimates and are often used to estimate GPP from remotely sensed data and process-based models. While, it suffers from an insufficient representation of several mechanism processes such as nitrogen deposition and CO_2 fertilization, and may imperfectly capture GPP inter-annual variability (Jung *et al* 2019). On the other hand, Schewe *et al* (2019) indicated that current terrestrial ecosystem models underestimate the effects of droughts on GPP due to the insufficient fitting of both human management and natural processes in the algorithms. Stocker *et al* (2019) found that satellite-based GPP estimates underestimate the effects of drought on GPP due to a lack of consideration of soil moisture impact on light use efficiency. As presented in our study, some investigations demonstrated that the VPM (Xiao *et al* 2004) and modified VPM (Zhang *et al* 2015a) generally outperform the other remotely sensed GPP estimates in capturing the effect of drought on GPP, due to including the impact of soil moisture on photosynthesis in the models (Zhang *et al* 2019, Pei *et al* 2020).

As such, the combination of GPP dataset from diverse and independent models can facilitate more reliable conclusions when evaluating the responses of GPP to drought at global and regional levels (Wu *et al* 2018, Sun *et al* 2021). Additionally, other mechanism processes such as CO2 fertilization and nutrients (i.e. phosphorus and nitrogen) on photosynthesis in the models should also be included (Du *et al* 2020).

6. Concluding remarks

Based on a remote sensing-driven GPP dataset, flux tower observation-based upscaling GPP, and components of terrestrial evapotranspiration (AET and PET) driven by GLEAM dataset estimates, we comprehensively examined the impacts of the SEDI on long term GPP variability over the ME for the period of 1982–2017. Focusing on dynamic changes of ecosystems' GPP, coupling analysis between the sGPPR and SEDI effect, and spatial heterogeneity. An ecosystem's ability to tolerate droughts was considered, along with whether various ecosystem types have varying responses. The main findings are as follows:

(a) The ecosystem productivity is sensitive to drought in semi-arid ecosystems, and the GPP's croplands and grasslands recorded the highest positive significant correlations and were more sensitive to the SEDI variability. Moreover, the ecosystem's GPP recorded a high decline during the 2008 extreme drought in the north of Iraq and the northeast of Syria.
(b) The proposed study reported that the ED-based index is more capable to capture the GPP variability and closely linked to drought than commonly used indices based on variables other than ED (e.g. SPEI).
(c) The VPM and FLUXCOM-based GPP correlated against the SEDI more closely than that of other GPP data in the ME. At the same time, the VPM and GLASS models-based GPP negative anomalies during the drought stress were higher than that of other GPP data.

However, there are some limitations to this study. First, the SEDI was implemented as the standardized difference between AET and PET at annual scale. More attention is required on the impacts of the SEDI and drought intensity and duration at the monthly and seasonal scale to explain this variance clearly. Secondly, vegetation productivity and ecosystem GPP could be indirectly and directly impacted by drought events. Besides drought-related solar radiation and precipitation, temperature, and wind speed factors, also other artificial variables, such as land use type could caused critical changes in vegetation GPP. This study did not investigate the effect of several crop types due to the lack of detailed information about the distribution of crop types spatially, which may drive to inconsistencies and uncertainty in the results. Thirdly, it is still difficult to precisely reproduce GPP. This limitation in GPP data may cause uncertain results when assessing the drought impacts on GPP via a few or divergent GPP parameters. The uncertainties in GPP by the selected models mainly produce from forcing parameters, structures of the models which simulating the stress of drought on photosynthesis and parameterization.

Further improvement on the ability of the models to estimate GPP under numerous conditions is required. This will improve the confidence in the assessment of drought hazards and their impacts on terrestrial carbon productivity. More attention is required on the impacts of drought intensity and duration at the monthly and seasonal scales to explain this variance clearly. Therefore, further studies should analyse the effects of droughts, besides anthropogenic activities and fire events, on terrestrial ecosystems. Those studies can consider ED-based drought indices to understand the potential dynamics affecting the spatial-temporal changes of the GPP in the ME. Moreover, they can consider the importance of detecting the direct concurrent and lagged impacts of droughts.

Data availability statement

The data that support the findings of this study are openly available at the following URL/DOI: http://doi.org/10.5281/zenodo.4540832.

Acknowledgments

The authors grateful for Nanjing University of Information Science and Technology and Lulea University of Technology for unlimited support. Authors would like to thank the FluxCom, GIMMS, VPM and GLASS and GLEAM teams for datasets sharing, we appreciate the provision of GPP dataset and components of terrestrial evapotranspiration products by them. This work was supported by the national natural science foundation of china (under Grants 41971340 and 4127141)

Conflicts of interest

The authors declare no conflict of interest.

Author contributions

Conceptualization, K A; methodology, K A; software, K A; formal analysis, K A; investigation, K A; data curation, K A and A M; writing—original draft preparation, K A, A M and A E; writing—review and editing, S M, and S S S; visualization, K A; supervision, N A and S B. All authors have read and agreed to the published version of the manuscript.

Appendix

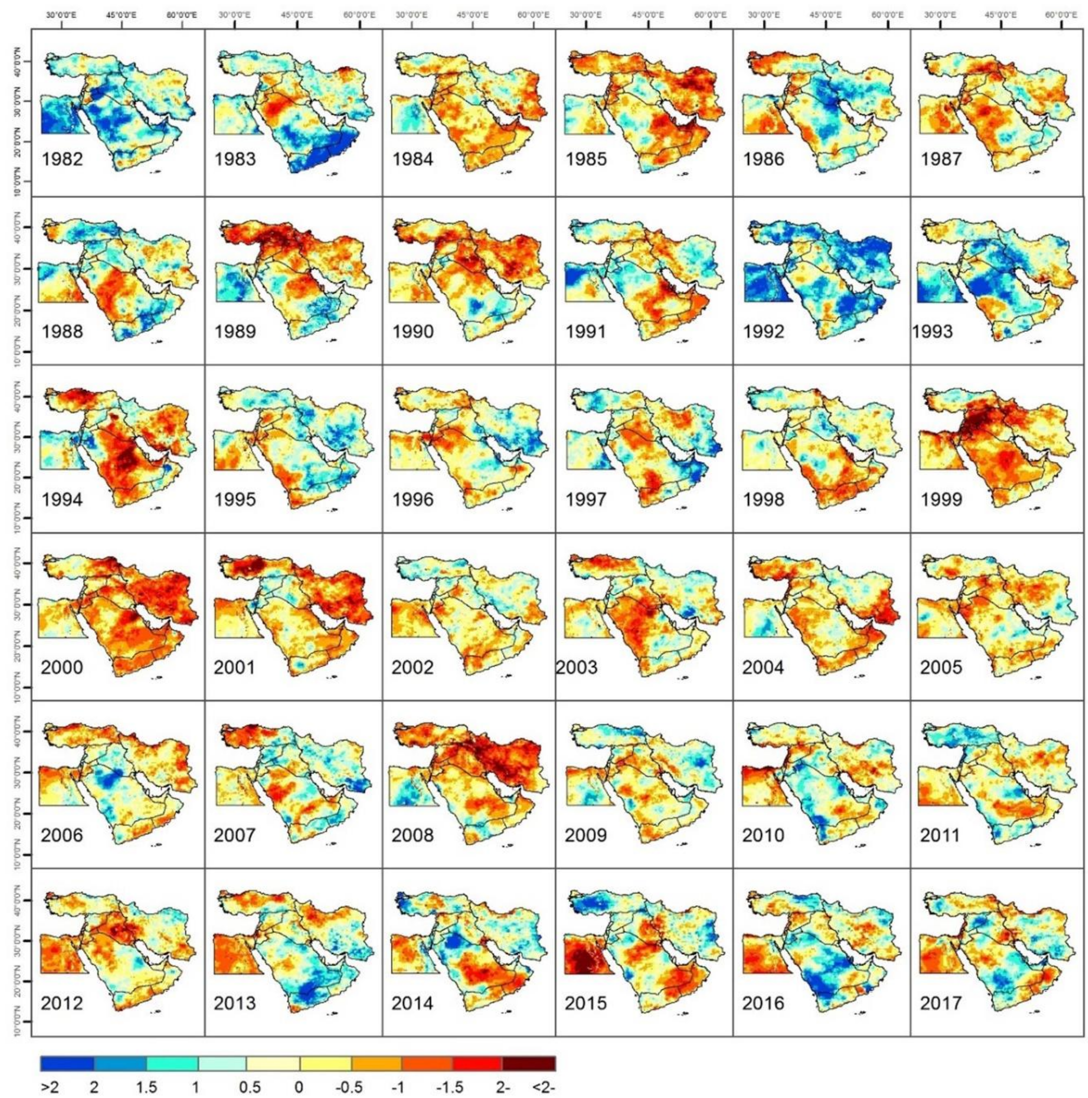

Figure A1. Spatial-temporal evolution of annual SEDI over the ME between 1982 and 2017.

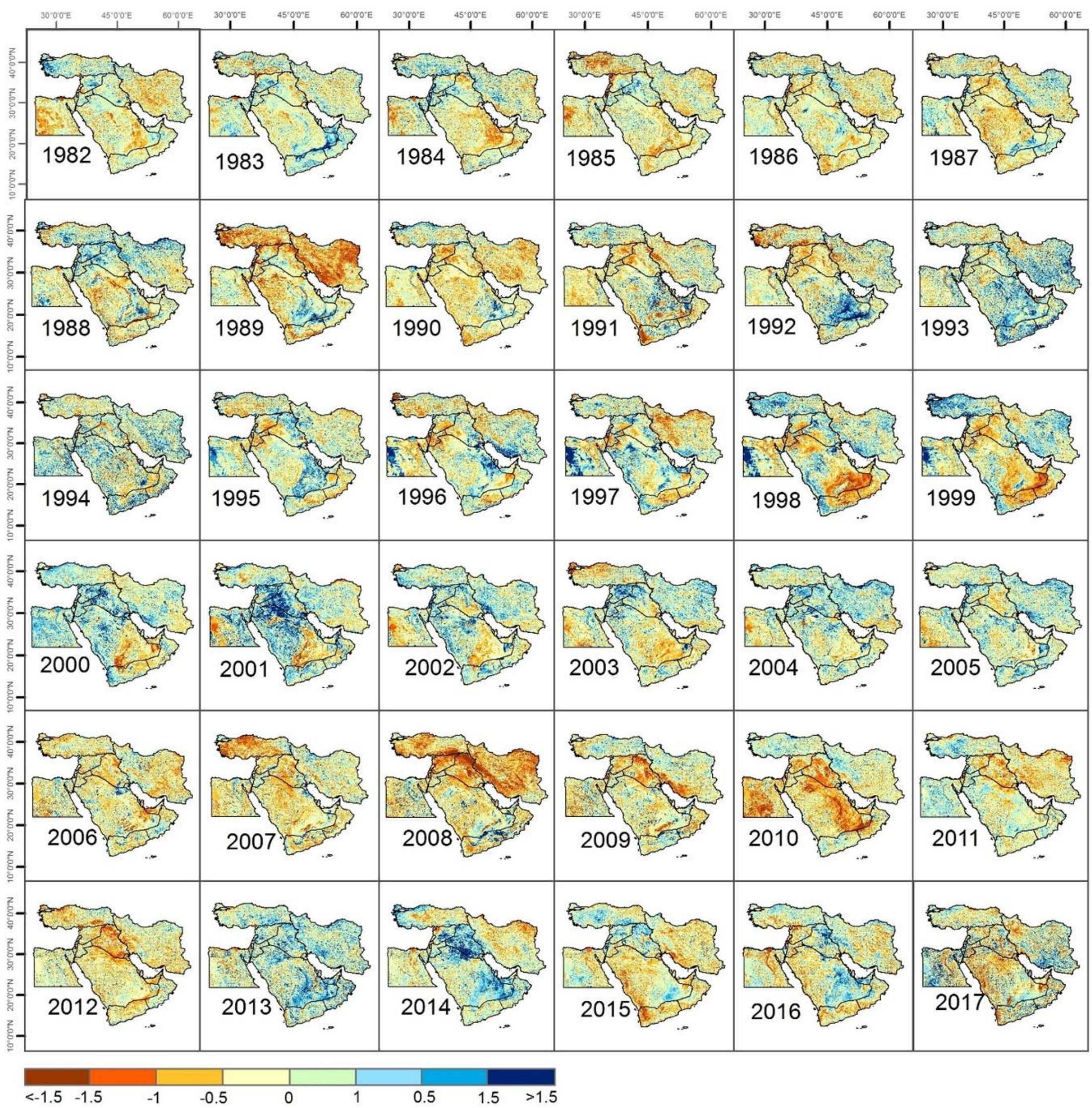

Figure A2. Spatial-temporal evolution of the annual GLASS-based sGPPR series over the ME between 1982 and 2017 at 0.05° arc degree spatial resolution.

Table B1. Percentage of area (%) from each land cover separately which has a significance correlation between the GLASS-based sGPPR and annual SEDI series from 1982 to 2017 at $p < 0.05$ (i.e. 95% confidence interval).

Countray	*Sig area	Croplands	Grassland	Area covered tree	Shrubs area	Sparse vegetation	Aquatic vegetation	Bare land
BHR	Sig (+)	—	—	—	—	—	—	0
	Sig (−)	—	—	—	—	—	—	0
EGY	Sig (+)	1.15	—	—	12.7	5.7	0.98	3.2
	Sig (−)	27.15	—	—	0	4	2.5	7.1
IRN	Sig (+)	14.3	17.6	19.8	15.75	16.1	10.4	8.1
	Sig (−)	1.12	0.7	0.5	0.8	1.25	2.25	1.3
IRQ	Sig (+)	29.6	30.6	32.4	28.3	20	7.4	10.9
	Sig (−)	0.5	0.2	0	0.44	0.43	5.4	0.5
ISR	Sig (+)	40.8	30.4	—	15	14.3	—	3.3
	Sig (−)	0	0	—	0	0	—	4.6
JOR	Sig (+)	16.5	0	—	—	4.1	—	4.3
	Sig (−)	0	0	—	—	3.4	—	7
KSA	Sig (+)	4.7	—	—	0	1.3	—	15.2
	Sig (−)	9.2	—	—	15.2	30.9	—	2.9
KWT	Sig (+)	—	—	—	—	0	—	7.4
	Sig (−)	—	—	—	—	0	—	0.3
LBN	Sig (+)	15	14.3	9.4	23.8	10	—	22.5
	Sig (−)	0	0	0	0	0	—	0
OMN	Sig (+)	0	—	—	3.6	3.1	—	7.5
	Sig (−)	0	—	—	2.4	6.25	—	2.1
PSE	Sig (+)	0	7.4	—	—	32.5	—	16.6
	Sig (−)	0	0	—	—	0	—	1.9
QAT	Sig (+)	11.1	—	—	—	—	—	7
	Sig (−)	—	—	—	—	—	—	1
SYR	Sig (+)	34	25	6.4	12.5	16.7	—	13.2
	Sig (−)	0.4	0	0	0	0.3	—	—
TUR	Sig (+)	30.5	21.2	21.3	31.8	18.8	29.4	17.8
	Sig (−)	0.5	0.9	1.1	1	0.6	0	1.2
UAE	Sig (+)	10.7	—	—	—	—	—	20.1
	Sig (−)	0	—	—	—	—	—	2
YEM	Sig (+)	0	0	—	—	—	—	7.8
	Sig (−)	41.8	0	—	—	—	—	6.1

Notes: (*) significance values (Sig+ and Sig−)

ORCID iDs

Karam Alsafadi https://orcid.org/0000-0001-8925-7918
Safwan Mohammed https://orcid.org/0000-0003-2311-6789

References

Alsafadi K, Mohammed S A, Ayugi B, Sharaf M and Harsányi E 2020 Spatial–temporal evolution of drought characteristics over Hungary between 1961 and 2010 *Pure Appl. Geophys.* **177** 3961–78

Alsafadi K and Bi S 2021 Standardized dataset of the ecosystem's gross primary productivity (sGPP) and the evapotranspiration deficit index (SEDI) for 1982–2017 over the Middle East [Data set] (Version 1) (Zenodo) (https://doi.org/10.5281/zenodo.4540832)

Anderegg W R, Flint A, Huang C Y, Flint L, Berry J A, Davis F W and Field C B 2015 Tree mortality predicted from drought-induced vascular damage *Nat. Geosci.* **8** 367–71

Barlow M, Zaitchik B, Paz S, Black E, Evans J and Hoell A 2016 A review of drought in the Middle East and southwest Asia *J. Clim.* **29** 8547–74

Beguería S, Vicente-Serrano S M and Angulo-Martínez M 2010 A multiscalar global drought dataset: the SPEIbase: a new gridded product for the analysis of drought variability and impacts *Bull. Am. Meteorol. Soc.* **91** 1351–4

Beguería S, Vicente-Serrano S M, Reig F and Latorre B 2014 Standardized precipitation evapotranspiration index (SPEI) revisited: parameter fitting, evapotranspiration models, tools, datasets and drought monitoring *Int. J. Climatol.* **34** 3001–23

Belgacem A O and Louhaichi M 2013 The vulnerability of native rangeland plant species to global climate change in the West Asia and North African regions *Clim. Change* **119** 451–63

Bozkurt D and Sen O L 2013 Climate change impacts in the Euphrates–Tigris basin based on different model and scenario simulations *J. Hydrol.* **480** 149–61

Cao S 2008 Why large-scale afforestation efforts in China have failed to solve the desertification problem *Environ. Sci. Technol.* **42** 1826–31

Chen G, Tian H, Zhang C, Liu M, Ren W, Zhu W and Lockaby G B 2012 Drought in the Southern United States over the 20th century: variability and its impacts on terrestrial ecosystem productivity and carbon storage *Clim. Change* **114** 379–97

Chen T, Werf G R, Jeu R D, Wang G and Dolman A J 2013 A global analysis of the impact of drought on net primary productivity *Hydrol. Earth Syst. Sci.* **17** 3885–94

Ciais P, Reichstein M, Viovy N, Granier A, Ogée J, Allard V and Valentini R 2005 Europe-wide reduction in primary productivity caused by the heat and drought in 2003 *Nature* **437** 529–33

Dai A 2011 Drought under global warming: a review *Wiley Interdiscip. Rev. Clim. Change* **2** 45–65

Deng L, Shangguan Z P and Sweeney S 2014 'Grain for Green' driven land use change and carbon sequestration on the Loess Plateau, China *Sci. Rep.* **4** 1–8

Du E *et al* 2020 Global patterns of terrestrial nitrogen and phosphorus limitation *Nat. Geosci.* **13** 221–26

Eamus D 2003 How does ecosystem water balance affect net primary productivity of woody ecosystems? *Funct. Plant Biol.* **30** 187–205

Elbeltagi A, Kumari N, Dharpure J K, Mokhtar A, Alsafadi K, Kumar M and Kuriqi A 2021 Prediction of combined terrestrial evapotranspiration index (CTEI) over large river basin based on machine learning approaches *Water* **13** 547

FAO 2014 Global land cover (GLC-SHARE) beta-release 1.0 database, land and water division, John Latham, Renato Cumani, Ilaria Rosati and Mario Bloise

Green J K, Seneviratne S I, Berg A M, Findell K L, Hagemann S, Lawrence D M and Gentine P 2019 Large influence of soil moisture on long-term terrestrial carbon uptake *Nature* **565** 476–9

Hameed M, Ahmadalipour A and Moradkhani H 2020 Drought and food security in the middle east: an analytical framework *Agric. For. Meteorol.* **281** 107816

Huang K, Zhang Y, Zhu J, Liu Y, Zu J and Zhang J 2016a The influences of climate change and human activities on vegetation dynamics in the Qinghai–Tibet plateau *Remote Sens.* **8** 876

Huang L, He B, Chen A, Wang H, Liu J, Lű A and Chen Z 2016b Drought dominates the interannual variability in global terrestrial net primary production by controlling semi-arid ecosystems *Sci. Rep.* **6** 1–7

Jardine C N 2003 Environmental challenges and greenhouse gas control for fossil fuel utilisation in the 21st century *Environ. Sci. Policy* **6** 395–6

Jiao W, Chang Q and Wang L 2019a The sensitivity of satellite solar-induced chlorophyll fluorescence to meteorological drought *Earth's Future* **7** 558–73

Jiao W, Tian C, Chang Q, Novick K A and Wang L 2019b A new multi-sensor integrated index for drought monitoring *Agric. For. Meteorol.* **268** 74–85

Jiao W, Wang L and McCabe M F 2021 Multi-sensor remote sensing for drought characterization: current status, opportunities and a roadmap for the future *Remote Sens. Environ.* **256** 112313

Jung M, Koirala S, Weber U, Ichii K, Gans F, Camps-Valls G, Papale D, Schwalm C, Tramontana G and Reichstein M 2019 The FLUXCOM ensemble of global land-atmosphere energy fluxes *Sci. Data* **6** 74

Jung M, Schwalm C, Migliavacca M, Walther S, Camps-Valls G, Koirala S and Reichstein M 2020 Scaling carbon fluxes from eddy covariance sites to globe: synthesis and evaluation of the FLUXCOM approach *Biogeosciences* **17** 1343–65

Kaniewski D, van Campo E and Weiss H 2012 Drought is a recurring challenge in the Middle East *Proc. Natl Acad. Sci.* **109** 3862–7

Karakani E G, Malekian A, Gholami S and Liu J 2021 Spatiotemporal monitoring and change detection of vegetation cover for drought management in the Middle East *Theor. Appl. Climatol.* **144** 299–315

Kim D and Rhee J 2016 A drought index based on actual evapotranspiration from the Bouchet hypothesis *Geophys. Res. Lett.* **43** 10–277

Kogan F 2002 World droughts in the new millennium from AVHRR-based vegetation health indices *Eos Trans. Am. Geophys. Union* **83** 557–63

Lei T, Wu J, Li X, Geng G, Shao C, Zhou H and Liu L 2015 A new framework for evaluating the impacts of drought on net primary productivity of grassland *Sci. Total Environ.* **536** 161–72

Lelieveld J, Hadjinicolaou P, Kostopoulou E, Chenoweth J, El Maayar M, Giannakopoulos C and Xoplaki E 2012 Climate change and impacts in the Eastern Mediterranean and the Middle East *Clim. Change* **114** 667–87

Li X, Liang S, Yu G, Yuan W, Cheng X, Xia J and Kato T 2013 Estimation of gross primary production over the terrestrial ecosystems in China *Ecol. Modell.* **261** 80–92

Liu L B, Gudmundsson L, Hauser M, Qin D H, Li S C and Seneviratne S I 2019 Revisiting assessments of ecosystem drought recovery *Environ. Res. Lett.* **14** 11

Liu W T and Kogan F N 1996 Monitoring regional drought using the vegetation condition index *Int. J. Remote Sens.* **17** 2761–82

Liu Y, Zhou Y, Ju W, Wang S, Wu X, He M and Zhu G 2014 Impacts of droughts on carbon sequestration by China's terrestrial ecosystems from 2000 to 2011 *Biogeosciences* **11** 2583–99

Margulis M E 2013 The regime complex for food security: implications for the global hunger challenge *Glob. Gov.* **19** 53–67

Martens B, Miralles D G, Lievens H, van der Schalie R, de Jeu R A M, Fernández-Prieto D, Beck H E, Dorigo W A and Verhoest N E C 2017 GLEAM v3: satellite-based land evaporation and root-zone soil moisture *Geosci. Model Dev.* **10** 1903–25

McKee T B, Doesken N J and Kleist J 1993 The relationship of drought frequency and duration to time scales *Proc. 8th Conf. on Applied Climatology* vol 17 (January) pp 179–83

Miralles D G, Holmes T R H, de Jeu R A M, Gash J H, Meesters A G C A and Dolman A J 2011 Global land-surface evaporation estimated from satellite-based observations *Hydrol. Earth Syst. Sci.* **15** 453–69

Mishra A K and Singh V P 2011 Drought modeling—a review *J. Hydrol.* **403** 157–75

Mohammed S, Alsafadi K, Al-Awadhi T, Sherief Y, Harsanyie E and El Kenawy A M 2020b Space and time variability of meteorological drought in Syria *Acta Geophys.* **68** 1877–98

Mohammed S, Alsafadi K, Daher H, Gombos B, Mahmood S and Harsányi E 2020a Precipitation pattern changes and response of vegetation to drought variability in the eastern Hungary *Bull. Natl Res. Centre* **44** 1–10

Mokhtar A, He H, Alsafadi K, Li Y, Zhao H, Keo S and He Q 2020 Evapotranspiration as a response to climate variability and ecosystem changes in southwest, China *Environ. Earth Sci.* **79** 1–21

Mokhtar A, He H, Alsafadi K, Mohammed S, He W, Li Y and Gyasi-Agyei Y 2021b Ecosystem water use efficiency response to drought over Southwest China *Ecohydrology* e2317

Mokhtar A, Jalali M, He H, Al-Ansari N, Elbeltagi A, Alsafadi K and Rodrigo-Comino J 2021a Estimation of SPEI meteorological drought using machine learning algorithms *IEEE Access* **9** 65503–23

Mu Q, Zhao M, Kimball J S, McDowell N G and Running S W 2013 A remotely sensed global terrestrial drought severity index *Bull. Am. Meteorol. Soc.* **94** 83–98

Narasimhan B and Srinivasan R 2005 Development and evaluation of soil moisture deficit index (SMDI) and evapotranspiration deficit index (ETDI) for agricultural drought monitoring *Agric. For. Meteorol.* **133** 69–88

Palmer W C 1965 Meteorological drought (vol 30) *Research Paper No.* 45 (US Department of Commerce, Weather Bureau) p 58

Pei F, Li X, Liu X and Lao C 2013 Assessing the impacts of droughts on net primary productivity in China *J. Environ. Manage.* **114** 362–71

Pei Y, Dong J, Zhang Y, Yang J, Zhang Y, Jiang C and Xiao X 2020 Performance of four state-of-the-art GPP products (VPM, MOD17, BESS and PML) for grasslands in drought years *Ecol. Inf.* **56** 101052

Piao S, Fang J, Zhou L, Zhu B, Tan K and Tao S 2005 Changes in vegetation net primary productivity from 1982 to 1999 in China *Glob. Biogeochem. Cycles* **19** GB2027

Prasad P V V and Staggenborg S A 2008 Impacts of drought and/or heat stress on physiological, developmental, growth, and yield processes of crop plants *Response of Crops to Limited Water: Understanding and Modeling Water Stress Effects on Plant Growth Processes* (Madison, WI: American Society of Agronomy, Crop Science Society of America, Soil Science Society of America) pp 301–55

Reichstein M, Bahn M, Ciais P, Frank D, Mahecha M D, Seneviratne S I and Wattenbach M 2013 Climate extremes and the carbon cycle *Nature* **500** 287–95

Rhee J, Im J and Carbone G J 2010 Monitoring agricultural drought for arid and humid regions using multi-sensor remote sensing data *Remote Sens. Environ.* **114** 2875–87

Saavedra C and Budd W W 2009 Climate change and environmental planning: working to build community resilience and adaptive capacity in Washington State, USA *Habitat Int.* **33** 246–52

Schewe J *et al* 2019 State-of-the-art global models underestimate impacts from climate extremes *Nat. Commun.* **10** 1005

Schwalm C R, Williams C A, Schaefer K, Arneth A, Bonal D, Buchmann N and Richardson A D 2010 Assimilation exceeds respiration sensitivity to drought: a FLUXNET synthesis *Glob. Change Biol.* **16** 657–70

Schwalm C R, Williams C A, Schaefer K, Baldocchi D, Black T A, Goldstein A H and Scott R L 2012 Reduction in carbon uptake during turn of the century drought in western North America *Nat. Geosci.* **5** 551–6

Smith W K, Reed S C, Cleveland C C, Ballantyne A P, Anderegg W R, Wieder W R and Running S W 2016 Large divergence of satellite and Earth system model estimates of global terrestrial CO_2 fertilization *Nat. Clim. Change* **6** 306–10

Stephenson N 1998 Actual evapotranspiration and deficit: biologically meaningful correlates of vegetation distribution across spatial scales *J. Biogeogr.* **25** 855–70

Stocker B D, Zscheischler J, Keenan T F, Prentice I C, Seneviratne S I and Peñuelas J 2019 Drought impacts on terrestrial primary production underestimated by satellite monitoring *Nat. Geosci.* **12** 264–70

Sun B, Zhao H and Wang X 2016 Effects of drought on net primary productivity: roles of temperature, drought intensity, and duration *Chin. Geogr. Sci.* **26** 270–82

Sun S, Du W, Song Z, Zhang D, Wu X, Chen B and Wu Y 2021 Response of gross primary productivity to drought time-scales across China *J. Geophys. Res. Biogeosci.* **126** e2020JG005953

Teuling A J, Seneviratne S I, Stöckli R, Reichstein M, Moors E, Ciais P and Wohlfahrt G 2010 Contrasting response of European forest and grassland energy exchange to heatwaves *Nat Geosci* **3** 722–7

Tramontana G, Jung M, Schwalm C R, Ichii K, Camps-Valls G, Ráduly B and Papale D 2016 Predicting carbon dioxide and energy fluxes across global FLUXNET sites with regression algorithms *Biogeosciences* **13** 4291–313

Tsakiris G and Vangelis H 2005 Establishing a drought index incorporating evapotranspiration *Eur. Water* **9** 3–11

van den Hoof C and Lambert F 2016 Mitigation of drought negative effect on ecosystem productivity by vegetation mixing *J. Geophys. Res. Biogeosci.* **121** 2667–83

Vicente-Serrano S M, Beguería S and López-Moreno J I 2010a A multiscalar drought index sensitive to global warming: the standardized precipitation evapotranspiration index *J. Clim.* **23** 1696–718

Vicente-Serrano S M, Beguería S, López-Moreno J I, Angulo M and El Kenawy A 2010b A new global 0.5 gridded dataset (1901–2006) of a multiscalar drought index: comparison with current drought index datasets based on the Palmer drought severity index *J. Hydrometeorol.* **11** 1033–43

Vicente-Serrano S M, Beguería S, Lorenzo-Lacruz J, Camarero J J, López-Moreno J I, Azorin-Molina C and Sanchez-Lorenzo A 2012 Performance of drought indices for ecological, agricultural, and hydrological applications *Earth Interact.* **16** 1–27

Vicente-Serrano S M, Miralles D G, Domínguez-Castro F, Azorin-Molina C, El Kenawy A, McVicar T R and Peña-Gallardo M 2018 Global assessment of the standardized evapotranspiration deficit index (SEDI) for drought analysis and monitoring *J. Clim.* **31** 5371–93

Vicente-Serrano S M, van der Schrier G, Beguería S, Azorin-Molina C and Lopez-Moreno J I 2015 Contribution of precipitation and reference evapotranspiration to drought indices under different climates *J. Hydrol.* **526** 42–54

Williams A P, Allen C D, Macalady A K, Griffin D, Woodhouse C A, Meko D M and McDowell N G 2013 Temperature as a potent driver of regional forest drought stress and tree mortality *Nat. Clim. Change* **3** 292–7

World Bank 2020 World development indicators database, population 2019 (available at: https://databank.worldbank.org/data/download/POP.pdf) (Accessed October 2020)

Wu X *et al* 2018 Spatiotemporal consistency of four gross primary production products and solar-induced chlorophyll fluorescence in response to climate extremes across CONUS in 2012 *J. Geophys. Res. Biogeosci.* **123** 3140–61

Wu Z, Wu J, He B, Liu J, Wang Q, Zhang H and Liu Y 2014 Drought offset ecological restoration program-induced increase in vegetation activity in the Beijing-Tianjin Sand Source Region, China *Environ. Sci. Technol.* **48** 12108–17

Xiao X, Hollinger D, Aber J, Goltz M, Davidson E A, Zhang Q and Moore B 2004 Satellite-based modeling of gross primary production in an evergreen needleleaf forest *Remote Sens. Environ.* **89** 519–34

Xiaobin G, Huanfeng S, Wenxia G and Liangpei Z 2014 Analysis of impacts of drought on GPP in Yunnan province based on MODIS products *2014 the Third Int. Conf. on Agro-Geoinformatics* (IEEE) (August) pp 1–4

Xu Z, Chen C, He J and Liu J 2009 Trends and challenges in soil research 2009: linking global climate change to local long-term forest productivity *J. Soils Sediments* **9** 83–88

Yao Y, Liang S, Qin Q and Wang K 2010 Monitoring drought over the conterminous United States using MODIS and NCEP Reanalysis-2 data *J. Appl. Meteorol. Climatol.* **49** 1665–80

Yi C, Ricciuto D, Li R, Wolbeck J, Xu X, Nilsson M and Zhao X 2010 Climate control of terrestrial carbon exchange across biomes and continents *Environ. Res. Lett.* **5** 034007

Yu Z, Wang J, Liu S, Rentch J S, Sun P and Lu C 2017 Global gross primary productivity and water use efficiency changes under drought stress *Environ. Res. Lett.* **12** 014016

Yuan W, Liu S, Zhou G, Zhou G, Tieszen L L, Baldocchi D and Wofsy S C 2007 Deriving a light use efficiency model from eddy covariance flux data for predicting daily gross primary production across biomes *Agric. For. Meteorol.* **143** 189–207

Zaitchik B F, Evans J P, Geerken R A and Smith R B 2007 Climate and vegetation in the Middle East: interannual variability and drought feedbacks *J. Clim.* **20** 3924–41

Zhang A, Jia G and Wang H 2019a Improving meteorological drought monitoring capability over tropical and subtropical water-limited ecosystems: evaluation and ensemble of the microwave integrated drought index *Environ. Res. Lett.* **14** 044025

Zhang L-X, Zhou D-C, Fan J-W and Hu Z-M 2015a Comparison of four light use efficiency models for estimating terrestrial gross primary production *Ecol. Modell.* **300** 30–39

Zhang L, Zhou D, Fan J, Guo Q, Chen S, Wang R and Li Y 2019b Contrasting the performance of eight satellite-based GPP models in water-limited and temperature-limited grassland ecosystems *Remote Sens.* **11** 1333

Zhang M, Wang K, Liu H, Zhang C, Wang J, Yue Y and Qi X 2015b How ecological restoration alters ecosystem services:

an analysis of vegetation carbon sequestration in the karst area of northwest Guangxi, China *Environ. Earth Sci.* **74** 5307–17

Zhang X, Chen N, Li J, Chen Z and Niyogi D 2017a Multi-sensor integrated framework and index for agricultural drought monitoring *Remote Sens. Environ.* **188** 141–63

Zhang X, Li M, Ma Z, Yang Q, Lv M and Clark R 2019c Assessment of an evapotranspiration deficit drought index in relation to impacts on ecosystems *Adv. Atmos. Sci.* **36** 1273–87

Zhang Y, Xiao X, Wu X, Zhou S, Zhang G, Qin Y and Dong J 2017b A global moderate resolution dataset of gross primary production of vegetation for 2000–2016 *Sci. Data* **4** 1–13

Zhao J, Hartmann H, Trumbore S, Ziegler W and Zhang Y 2013 High temperature causes negative whole-plant carbon balance under mild drought *New Phytol.* **200** 330–9

Zhao M and Running S W 2010 Drought-induced reduction in global terrestrial net primary production from 2000 through 2009 *Science* **329** 940–3

Zheng Y, Shen R, Wang Y, Li X, Liu S, Liang S and Yuan W 2020 Improved estimate of global gross primary production for reproducing its long-term variation, 1982–2017 *Earth Syst. Sci. Data* **12** 2725–46

Zhu X, Liu Y, Xu K and Pan Y 2021 Effects of drought on vegetation productivity of farmland ecosystems in the Drylands of Northern China *Remote Sens.* **13** 1179